Natural Resources, 2017, 8, 445-459
http://www.scirp.org/journal/nr
ISSN Online: 2158-7086
ISSN Print: 2158-706X

Synthesis and Characterization of a $[Li_{0+x}Mg_{2-2x}Al_{1+x}(OH)_6][Cl{\cdot}mH_2O]$ Solid Solution with X = 0 - 1 at Different Temperatures

A. Niksch, H. Pöllmann

Mineralogy/Geochemistry, Institute for Geosciences and Geography, University of Halle, Halle, Germany
Email: anton.niksch@geo.uni-halle.de

How to cite this paper: Niksch, A. Pöllmann, H. (2017) Synthesis and Characterization of a $[Li_{0+x}Mg_{2-2x}Al_{1+x}(OH)_6][Cl{\cdot}mH_2O]$ Solid Solution with X = 0 - 1 at Different Temperatures. *Natural Resources*, **8**, 445-459.
https://doi.org/10.4236/nr.2017.86029

Received: March 16, 2017
Accepted: June 25, 2017
Published: June 28, 2017

Abstract

The synthesis of a novel Li^+ /Mg^{2+} /Al^{3+} containing layered double hydroxide (LDH) by using a hydrothermal synthesis route is represented in this work. The autoclaves were heated up to 100˚C, 120˚C, 140˚C and 160˚C for 10 h and 48 h with a water to solid ratio (W/S) of 15:1. The physicochemical properties of the synthesized LDHs were investigated by X-ray powder diffraction (PXRD), fourier transform infrared spectroscopy (FTIR), thermo gravimetric and differential thermal analysis (TG-DTA), inductively coupled plasma optical emission spectroscopy (ICP-OES) and scanning electron microscopy (SEM). The formation of a solid solution phase depends strongly on the composition of the reactants and the synthesis temperature. Using an exact stoichiometric ratio of Li^+/Mg^{2+}/Al^{3+} resulted in the synthesis of amorphous phases without producing plenty of crystalline amounts of the expected solid solutions while using higher temperatures than 140˚C resulted in a formation of AlO(OH). To avoid the formation of an Al containing amorphous phase or an AlO(OH) crystalline phase, the stoichiometric ratio of Li^+ was changed. The results show solid solutions with the formula $[Li_{0+x}Mg_{2-2x}Al_{1+x}(OH)_6][Cl{\cdot}mH_2O]$ with $X \geq 0.9$. The lattice parameters and chemical compositions for solid solutions with different compositions were determined and the pure solid solution with the highest amount of Mg (x = 0.9) is $[Li_{0.9}Mg_{0.2}Al_{1.9}(OH)_6][Cl{\cdot}0.50H_2O]$ with the lattice parameters ***a*** = 5.1004(4) Å, ***c*** = 15.3512(1) Å, V = 345.844(9) Å³. For X < 0.9 two separate phases, a Mg^{2+} and a Li^+ dominated solid solution, are coexistent.

Keywords

Lithium LDH, Magnesium LDH, Solid Solution, X-Ray Powder Diffraction

1. Introduction

Layered double hydroxides (LDHs) consist of alternate positively charged mixed metal hydroxide layers and negative charged interlayer anions. The stoichiometry of these materials can be formulated as $[M^{z+}_{1-x}M^{3+}_{x}(OH)_2]^{p+}[(A^{n-})_{p/n}\cdot mH_2O]$ with z = 2, M = bi- and trivalent metallic elements, A = organic or inorganic anions and m = amount of interlayer H_2O depending on the temperature, relative humidity and hydration level [1]. A special case is $M^{z+} = Li^+$(z = 1) and $M^{3+} = Al^{3+}$. The ratio between Li and Al is always 1:2 [2] while the ratio between M^{z+} and M^{3+} (z = 2) can vary strongly [3] depending on which M^{2+} ion or synthesis parameters are used. These layered materials are able to intercalate negatively charged and neutral molecules or exchange the interlayer anion with organic [4] [5] [6] [7] [8] or inorganic [3] [9] anions of different sizes or charges. The $[M^{z+}_{1-x}M^{3+}_{x}(OH)_2]^{p+}$ main layer remains stable and is not capable of ion exchange once it is formed.

Two well-known and described LDHs are $[LiAl_2(OH)_6]$ $[Cl\cdot mH_2O]$ [2] [9] [10] and $[Mg_2Al(OH)_6]$ $[Cl\cdot mH_2O]$ [11]. Both compounds are generally synthesized by a direct reaction of a LiXor MgX_2(X = Cl^-, OH^-, NO_3^-, etc) with $Al(OH)_3$[2/4]or by a hydrothermal reaction with higher temperatures and pressures [1].

The structure of $Al(OH)_3$is built up of double layered sheets of hexagonally packed O atoms. Two thirds of the octahedral holes are occupied by Al atoms. Using LiX as the reaction partner leads to the formation of $[LiAl_2(OH)_6]$ $[X\cdot mH_2O]$ with Li^+ cations entering the vacancies in the aluminum hydroxide layers and A entering the interlayer space [1] [9]. The structure of the resulting Li-LDH depends directly on the structure of the used aluminium hydroxide. Syntheses using gibbsite as starting material leads to Li-LDHs with hexagonal symmetry, while reactions with bayerite or nordstrandite produce LDHs with rhombohedra symmetry [1] [10] [12]. In the brucite-like structure of $[Mg_2Al(OH)_6][X\cdot mH_2O]$, Mg^{2+} is octahedrally coordinated to six OH^- anions. These octahedrons share edges and form thereby a layer. Substituting Mg^{2+} with a trivalent ion like Al^{3+} leads to a positive charge which can be compensate by interlayer anions [11]. $[Mg_2Al(OH)_6][X\cdot mH_2O]$ can also be rhombohedra or hexagonal [13] [14]. The pure $[Mg_2Al(OH)_6]$ $[X\cdot mH_2O]$ phase produced within this work was hexagonal (P6/m).

Almost all publications concerning the interlayer anion exchange or the synthesis and physicochemical properties use a combination of M^{z+} (z = 1 or 2) + M^{3+} in the main layer with a variation of two different elements [3] [5] [15]-[20]. The aim of this research is to invent a novel solid solution by adding a Me^{2+} cation (Mg^{2+}) into the structure of a Li-LDH. The distance between Li^+ and O^{2-} ions in a $[LiAl_2(OH)_6]$ $[Cl\cdot mH_2O]$ LDH is 2.129Å and between Al^{3+} and O^{2-} 1.926Å [2]. In a $[Mg_2Al(OH)_6][Cl\cdot mH_2O]$ LDH, Mg^{2+} and Al^{3+} ions occupy the same positions with the same distance of 2.013Åbetween the cations and O^{2-} [21]. Comparing both structures and the bonding distances, it should be possible for Mg^{2+} ions to occupy the Al^{3+} and the Li^+ position in the solid solution.

2. Experimental

2.1. Reagents

The starting materials for this work were LiCl (ROTH, purity ≥ 99%), $MgCl_2 \cdot 6H_2O$ (AppliChem ≥ 99%), $AlCl_3 \cdot 6H_2O$ (Serva ≥ 98%) and NaOH (Fluka ≥ 97%). XRD investigations and loss of ignition (LOI) were done with all chemicals to exclude contaminations and determine the amount of crystal water.

2.2. Measurements

APAN anlytical X'PERT³ Powder diffractometer with Pixcel detector and a Cu radiation (45 kV/40 mA) was used for the X-ray powder diffraction (XRD). The samples were prepared with back loading procedure and recorded from 5˚ - 70˚2θ with a step width of 0.017˚2θ and a irradiation time per step of 19.685 s. Thermogravimetric analysis and differential thermal analysis (TGA/DTA) for the dried samples (relative humidity (RH) 35%) were done simultaneously by the 320U from Seiko Instruments under nitrogen flow and a 2.5 K/min heating rate between 25˚C - 1000˚C. Fourier transform infrared spectra (FTIR) were recorded by an IFS 55 Equinox FTIR spectrometer from Bruker (400 - 4000 cm^{-1}). The scanning electron microscope (SEM) pictures were taken by a JOEL 640 SEM and the chemical compositions of the samples were proven by a Horiba Ultima2 inductively coupled plasma optical emission spectroscopy (ICP-OES).

2.3. Synthesis

All mixtures of the initial components were prepared in a glove box with nitrogen atmosphere to avoid carbonatization. The synthesis were carried out in 35 ml PTFE-lined stainless-stealautoclaves [1] by adding solutions of LiCl, $MgCl_2 \cdot 6H_2O$ and $AlCl_3 \cdot 6H_2O$with a W/S of 15: 1(a total of 1 g salts with 15 ml deionized/decarbonized water) and 5M NaOH until an alkaline pH (8.5) was reached and heating it up 10 h and 48 h. A series of experiments with different temperatures, synthesis times and pH were carried out to achieve the best result for a pure solid solution. The synthesis temperature was varied between 100˚C, 120˚C, 140˚C and 160˚C and two different synthesis times (10 h and 48 h) and pH (8.5/9.5) were tested. To synthesize pure $[Mg_2Al(OH)_6][Cl \cdot mH_2O]$ an exact ratio of 2 mol Mg^{2+}: 1 mol $Al^{3+}$was chosen andthe pure $[LiAl_2(OH)_6][Cl \cdot mH_2O]$ was prepared by adding the Li^+ and Al^{3+} salts in an exact 1 mol : 2 mol ratio. While the Mg containing LDH was prepared without problems, the Li LDH showed a high proportion of an amorphous phase. ICP-OES investigations stated that only 20% of Li^+ was incorporated in the LDH structure leaving 80% of Li^+ in the solution and the so remaining excess of Al^{3+} as an amorphous phase. A five times higher concentration of Li^+ [10], as required by stoichiometry for the preparation of the pure $[LiAl_2(OH)_6][Cl \cdot mH_2O]$ LDH, was necessary to compensate the 80 % lack of Li^+ in the solid state.

After the synthesis of pure $[Mg_2Al(OH)_6][Cl \cdot mH_2O]$, the amount of Li^+ was increased and the amount of Mg^{2+} was reduced in 10 mol% (X = 0.1) steps until

100 mol% Li ($[LiAl_2(OH)_6][Cl{\cdot}mH_2O]$) was reached. The products were filtered, washed with 30 ml deionized water and dried (RH 35%) until a constant mass was reached.

The mineralogical phases were determined by X-ray powder diffraction, the chemical compositions of the products by ICP-OES using the filtrate and the synthesis products dissolved in HNO_3 [11] [16].

3. Results and Discussion

3.1. Stoichiometric Composition

First experiments were carried out at 100˚C, pH 8.5, 10 h synthesis time and a W/S ratio of 15:1. Using an exact stoichiometric ratio of $Li^+/Mg^{2+}/Al^{3+}$ resulted in the synthesis of a high proportion of an amorphous phase with a small amount of a crystalline solid solution. After drying at 80˚C, XRD analysis showed a recrystallized $Al(OH)_3$ phase next to the LDH main phase.

Investigations of the filtered solutions and the dissolved products with ICP-OES stated that, independent from the Mg reactant amount, 99% - 100% of Mg^{2+} but only 20% of Li^+ were build-in into a LDH phase. The other 80% of Li^+ remained in the solution. Due to the stoichiometric reactant ratio the leftover Li^+ ions in the solution are leading to leftover Al^{3+}. These Al^{3+} ions formed $Al(OH)_3$ in the basic environment. Using higher temperatures (up to 160˚C) or synthesis times (48 h) showed no positive effect for the crystallization of a pure LDH phase. Increasing pH from 8.5 to 9.5 resulted in a slightly higher amount of a crystalline phase.

3.2. Composition with Increased Li^+ Content

After a five times increasement of the stoichiometric amount of Li^+ (equal to the pure Li-LDH synthesis), with a resulting ratio of Li: Mg: Al = 5: 1: 1, a pure crystalline LDH phase could be achieved. ICP-OES studies stated that >99% of Mg^{2+} and Al^{3+} and the needed 20 % of the five times higher Li^+ concentration were build-in into the crystalline phase.

3.2.1. PXRD Analysis

By increasing X from 0 to 1 in 0.1 mol steps in $[Li_{0+x}Mg_{2-2x}Al_{1+x}(OH)_6][Cl{\cdot}mH_2O]$, the amount of $Mg^{2+}$is decreased and replaced by Al^{3+} and Li^+. This leads to a change of the lattice parameter ***a*** and the cell volume. Comparing the ion radii of Mg^{2+} (0.65 Å) with Li^+ (0.60 Å) and Al^{3+} (0.50 Å) it is to be expected that the lattice parameter ***a*** starts to decrease with higher Li^+/Al^{3+}content [7]. A dependent change in the lattice parameter ***c*** or the basal reflections (00*l*) is not visible. By means of the (110)/(112) and (300)/(302) peaks, it is easily possible to distinguish the two different phases $[Mg_2Al(OH)_6][Cl{\cdot}mH_2O]$ (P6/m) and $[LiAl_2(OH)_6][Cl{\cdot}mH_2O]$ ($P6_3/m$). Starting with X = 0 (pure $[Mg_2Al(OH)_6][Cl{\cdot}mH_2O]$ phase) a separation in two phases is visible between X = 0.1 and X = 0.8 (**Figure 1** and **Figure 2**). The ˚2Θ positions of the 110/112peaks at X = 0.1 - 0.8 show a peak shift to higher ˚2Θ angles in relation to the pure $[Mg_2Al(OH)_6][Cl{\cdot}mH_2O]$

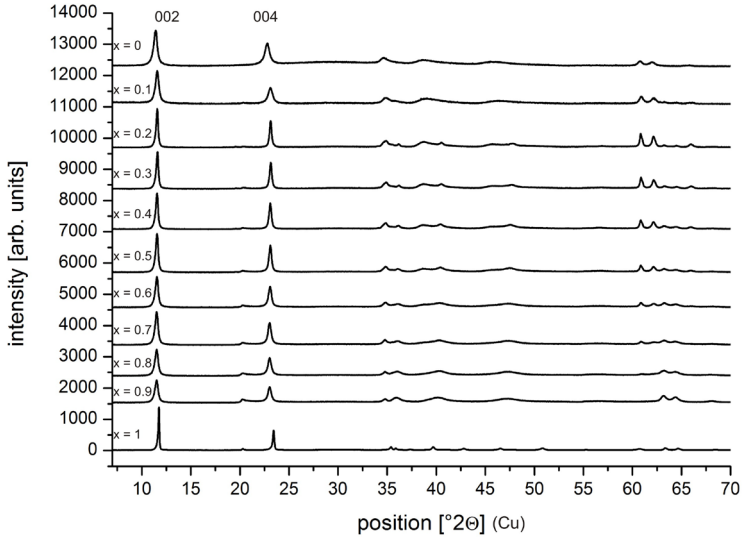

Figure 1. XRD pattern of the test series with X for$[Li_{0+x}Mg_{2-2x}Al_{1+x}(OH)_6][Cl{\cdot}mH_2O]$ (120˚C/10 h) showing no visible phase separation at the (002)/(004) main peaks but two coexisting phases at higher ˚2Θ angle (60 - 65).

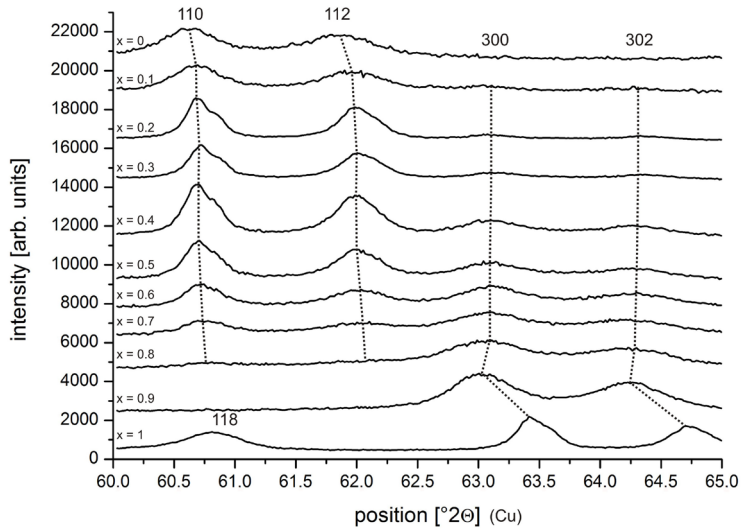

Figure 2. XRD pattern in the range of 60˚ to 65 ˚2Θ of the test series with X for $[Li_{0+x}Mg_{2-2x}Al_{1+x}(OH)_6][Cl{\cdot}mH_2O]$. The pattern for x = 0.1 until x = 0.8 show two different phases.

phase (**Figure 2** and **Figure 3**) which is also visible in the lattice parameter (**Table 1**). This shift increases with higher Li^+ reactant amounts, which indicates Mg dominated solid solutions with different Li^+/Mg^{2+} ratios.

While the (110)/(112) peaks are completely erased for X = 0.9, the (300)/(302) peaks shifted and the solid solution hasa different lattice parameter compared to $[LiAl_2(OH)_6][Cl{\cdot}mH_2O]$ at X = 1 [2] (**Figure 2** and **Figure 3**, **Table 1**). The lattice parameter ***a*** is closeto the calculated ideal position of a solid solution. Between X = 0.1 - 0.8 the (300)/(302) peaks have nearly the same position which is shifted to lower ˚2Θ angles and the lattice parameter are also nearly constant. This indicates a stable Li dominated solid solution with a defined amount of

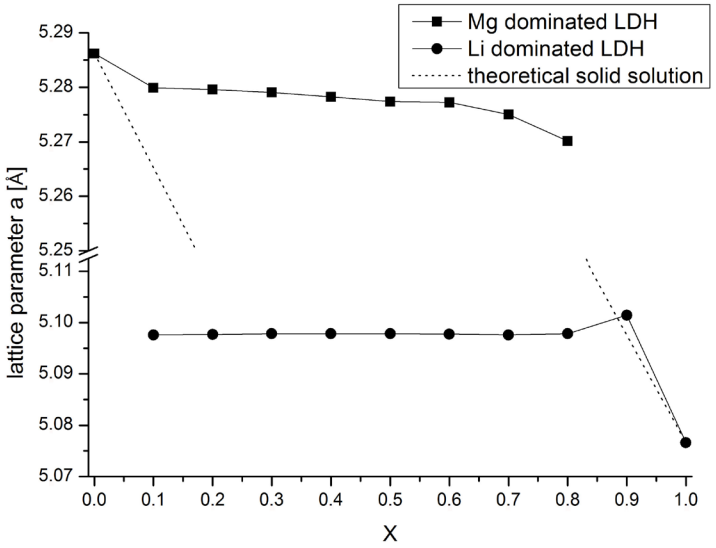

Figure 3. Lattice parameter **a** of two different phases with X for $[Li_{0+x}Mg_{2-2x}Al_{1+x}(OH)_6][Cl{\cdot}mH_2O]$. The black dashed line shows the theoretical lattice parameter of the solid solutions.

Table 1. Pawley fitted lattice parameter **a/c** for $[Mg_2Al(OH)_6][Cl{\cdot}mH_2O]$ (X = 0), $[LiAl_2(OH)_6][Cl{\cdot}mH_2O]$ (X = 1) and the split Li and Mg dominated solid solutions.

X	lattice parameter **a** [Å]		lattice parameter **c** [Å]	
	phase 1 (Mg dominated)	phase 2 (Li dominated)	phase 1 (Mg dominated)	phase 2 (Li dominated)
0	5.2862 (1)	-	15.4231 (3)	
0.1	5.2784 (1)	5.0966 (1)	15.3655 (2)	15.3650 (4)
0.2	5.2795 (9)	5.0976 (7)	15.3591 (9)	15.3582 (3)
0.3	5.2790 (3)	5.0978 (2)	15.3589 (4)	15.3593 (1)
0.4	5.2782 (5)	5.0978 (3)	15.3599 (2)	15.3596 (6)
0.5	5.2773 (8)	5.0978 (2)	15.3581 (5)	15.3584 (4)
0.6	5.2772 (3)	5.0977 (4)	15.3612 (1)	15.3609 (1)
0.7	5.2750 (3)	5.0970 (6)	15.3644 (1)	15.3647 (9)
0.8	5.2701 (6)	5.0978 (2)	15.3608 (3)	15.3602 (2)
0.9	-	5.0978 (9)	-	15.3601 (8)
1	-	5.0766 (2)	-	15.3425 (3)

Mg^{2+} independent from the Mg^{2+} reactant amount. The miscibility gap for X = 0.1 - 0.8 was observed at all tested synthesis temperatures (100˚C - 160˚C) and times (10 h/48 h).

To synthesize pure solid solution phases, test series between X = 0.9 and X = 1 (in 0.02 mol steps) were conducted. XRD results show a single mineral phase with h0l peak shifts (Figure 4 and Figure 5). This peak shifts follow nearly the

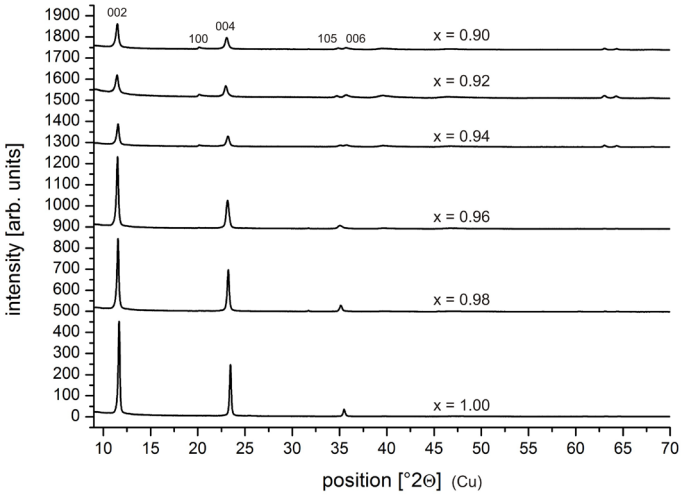

Figure 4. XRD pattern of the test series with X = 0.9 - 1 for$[Li_{0+x}Mg_{2-2x}Al_{1+x}(OH)_6][Cl{\cdot}mH_2O]$. X was increased in 0.02 mol steps (120˚C/10 h). Due to a preferred orientation of 00l, the (100) and (105) peak is no longer visible for X = 0.96; 0.98; 1.

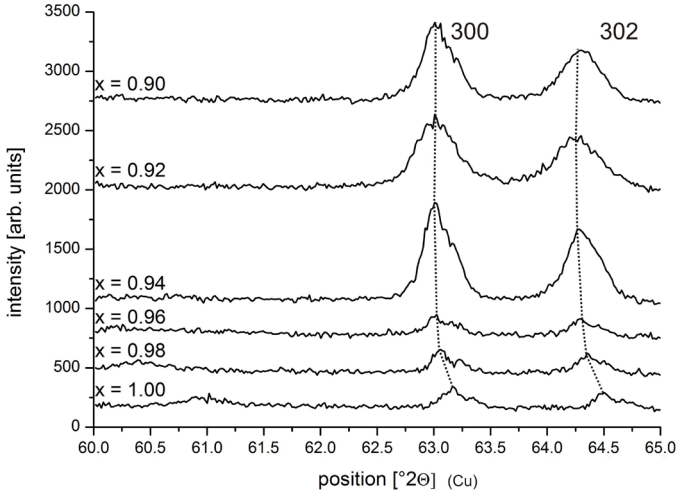

Figure 5. XRD pattern in the range of 60˚ to 65 ˚2Θ of the test series with series with X = 0.9 - 1 for $[Li_{0+x}Mg_{2-2x}Al_{1+x}(OH)_6][Cl{\cdot}mH_2O]$ with marked peaks. A shift for the (300) and (302) peaks is visible.

calculated shifts for the solid solutions (**Figure 6**). These experiments were also done at four different temperatures (100˚C, 120˚C, 140˚C, 160˚C). Although there is a shift difference depending on the temperature (**Figure 6**), no phase separation was observed for all investigated solid solutions (**Figure 5**).

The optimal results for a pure solid solution phase were achieved at 120˚C/10 h synthesis time/pH 9.5 and W/S ratio 15:1 (**Figure 6**/**Table 2**). The measured lattice parameters ***a*** differ only slightly from the calculated and the lattice parameters ***c*** are nearly constant (**Table 2**).

The products were fitted by Pawley fit and the space group was determined as $P6_3/m$ for all pure solid solutions up to X = 0.9. Investigations of the lattice parameter ***a*** show a straight increase from ~5.08Å (X = 0) [8] to ~5.10Å (X = 0.1) as calculated (**Figure 6**/**Table 2**).

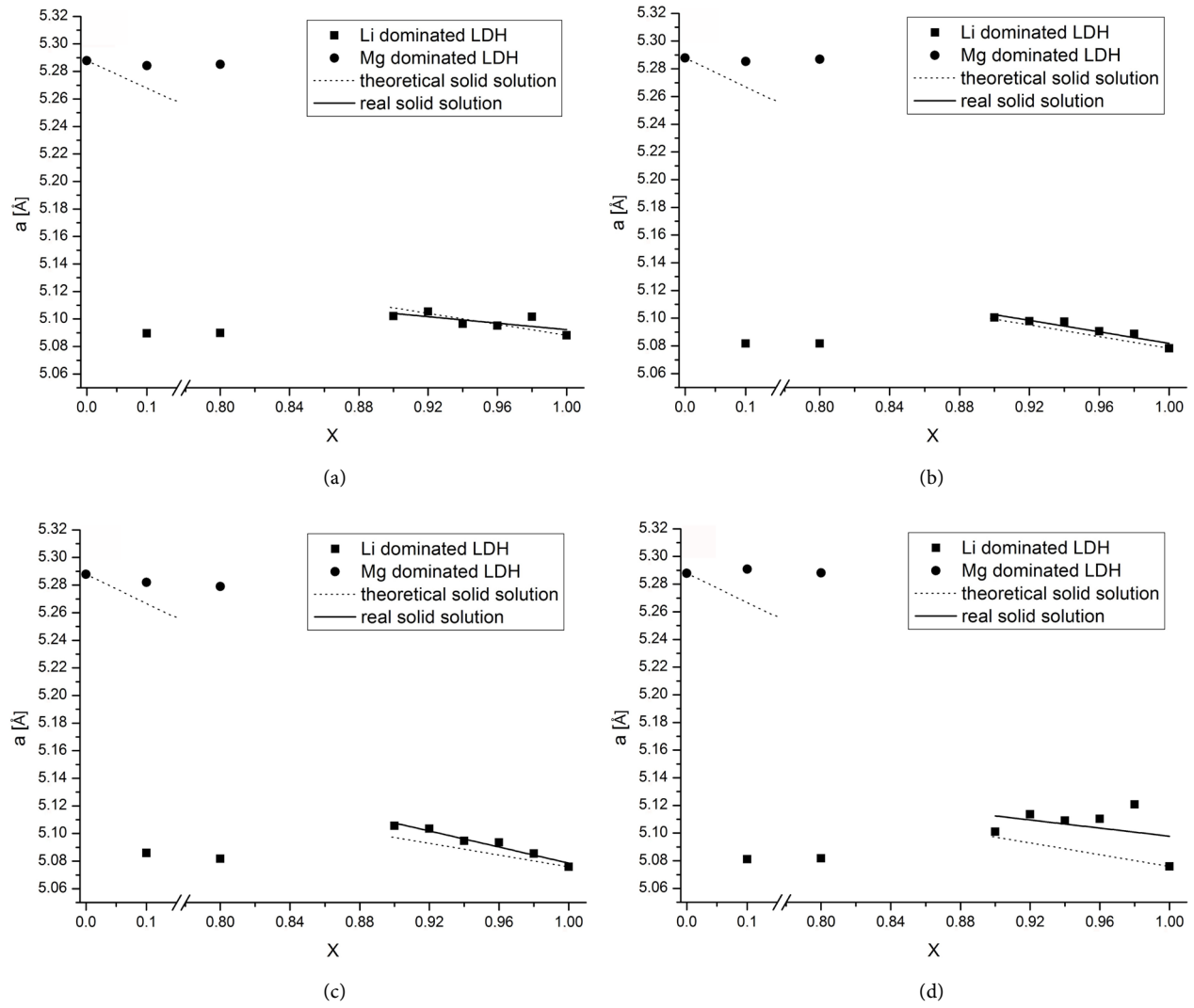

Figure 6. Theoretical and measured lattice parameter **a** for the solid solutions with X = 0.1, 0.8, 0.9 - 0.98 for $[Li_{0+x}Mg_{2-2x}Al_{1+x}(OH)_6]$ $[Cl{\cdot}mH_2O]$and the pure Mg/Li LDH at (a) 100˚C; (b) 120˚C; (c) 140˚C; (d) 160˚C. For X = 0.1/0.8 two separated LDH phases are visible.

Table 2. Theoretical and measured/fitted lattice parameter (a) and (c) for the solid solutions with X = 0.9 - 0.98 and $[LiAl_2(OH)_6][Cl{\cdot}0.51H_2O]$ at X = 1 (120˚C/10 h/pH 9.5/W/S 15: 1).

X	theoretical lattice parameter a [Å]	measured lattice parameter a [Å]	measured lattice parameter c [Å]	Measured cellvolume [Å]³	spacegroup
0.9	5.0962	5.1004 (4)	15.3512 (1)	345.844 (9)	$P6_3/m$
0.92	5.0922	5.0978 (3)	15.3602 (3)	345.694 (9)	$P6_3/m$
0.94	5.0881	5.0975 (1)	15.3563 (7)	345.566 (5)	$P6_3/m$
0.96	5.0840	5.0906 (9)	15.3497 (1)	344.483 (5)	$P6_3/m$
0.98	5.0799	5.0886 (8)	15.3550 (3)	344.331 (7)	$P6_3/m$
1	5.0759	5.0783 (8)	15.3483 (4)	342.789 (5)	$P6_3/m$

3.2.2. ICP-OES Analysis

To determine the chemical formula, all products were completely dissolved in-suprapur 65% nitric acid and investigated with ICP-OES [11] [16]. The results were used to calculatethe LDH formulas (Table 4). These calculations also stated a maximum content of an amorphous phase of <1%. Recrystallization tests showed no Al containing phases. Synthesis temperatures higher than 140˚C led to a destabilization of the LDH phase and the formation of AlO(OH) (Figure 7). The test series with 160˚C were repeated several times producing always AlO(OH) next to the LDH. Calculations showed an Al containing amorphous phase and crystalline AlO(OH) proportion of 10 % to 90 % (Table 3). The resulting lack of Al^{3+} in the solid solution leads to LDH phases with a higher Mg/Al ratio than 2:1 and therefore to the formation of a LDH with higher Mg^{2+} amounts next to the AlO(OH) phase (Figure 6(d)).

Table 3. Proportion of the amorphous phase/AlO(OH) depending on the synthesis temperature.

T [˚C]	Al containing amorphous phase/[%]
100	<1
120	<1
140	<1
160	>10

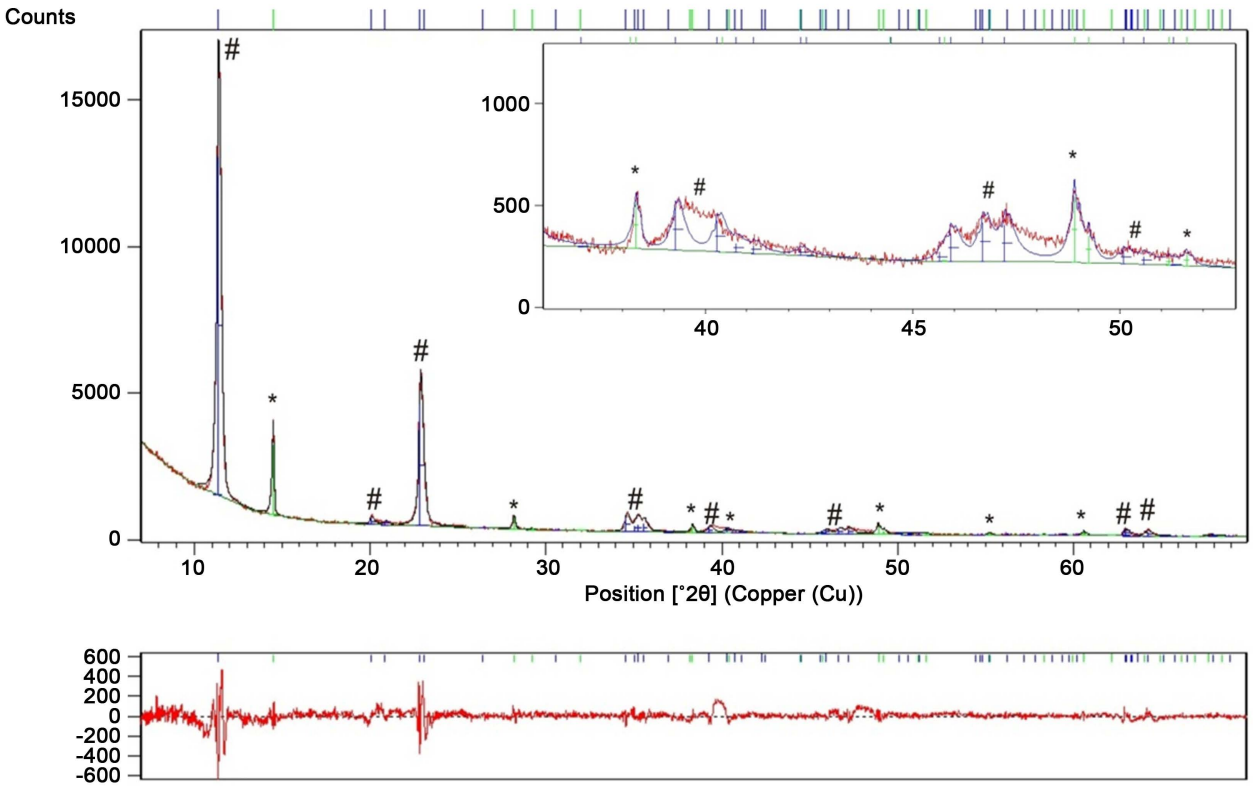

Figure 7. Pawley fit of a solid solution $[Li_{0.90}Mg_{0.25}Al_{1.87}(OH)_6]$][Cl·mH_2O] synthesized at 160˚C. A phase of AlO(OH) (*) is visible next to the solid solution (#). The broadening at 40˚ and 47˚ ˚2θ(small picture) is interpreted as stacking faults [7].

3.2.3. Thermal Analysis

The amount of interlayer water was determined by TG/DTA for $[LiAl_2(OH)_6][Cl{\cdot}0.50H_2O]$, $[Mg_2Al(OH)_6][Cl{\cdot}0.55H_2O]$and all pure solid solutions (Table 4). An example for the Li-LDH, Mg-LDH and the solid solution with the highest Mg^{2+} amount $[Li_{0.9}Mg_{0.2}Al_{1.90}(OH)_6][Cl{\cdot}0.51H_2O]$ is shown in Figure 8. Comparing the solid solution with the pure Li- and Mg-LDH, there is a high similarity in mass loss and exothermal reaction. The mass loss at 75˚C - 100˚C is caused by the removal of intercalated interlayer water [2] [6]. With 4.5% for the pure Li-LDH, 4.2% for the solid solution and 4.7% for the pure Mg-LDH it corresponds with the loss of 0.50 to 0.55 water per formula unit of the LDHs. While the differential thermal analysis of the pure Li- and Mg-LDH show a single endothermic reaction at 275˚C - 325˚C, the solid solution shows two (260˚C and 320˚C). At this temperature, the LDH starts to dehydroxylate which results in the destruction of the metal hydroxide main layer [2] [6] [7] [11]. Combining Li^+ and Mg^{2+} with Al^{3+} in the main layer leads to a two-step dehydroxylation.

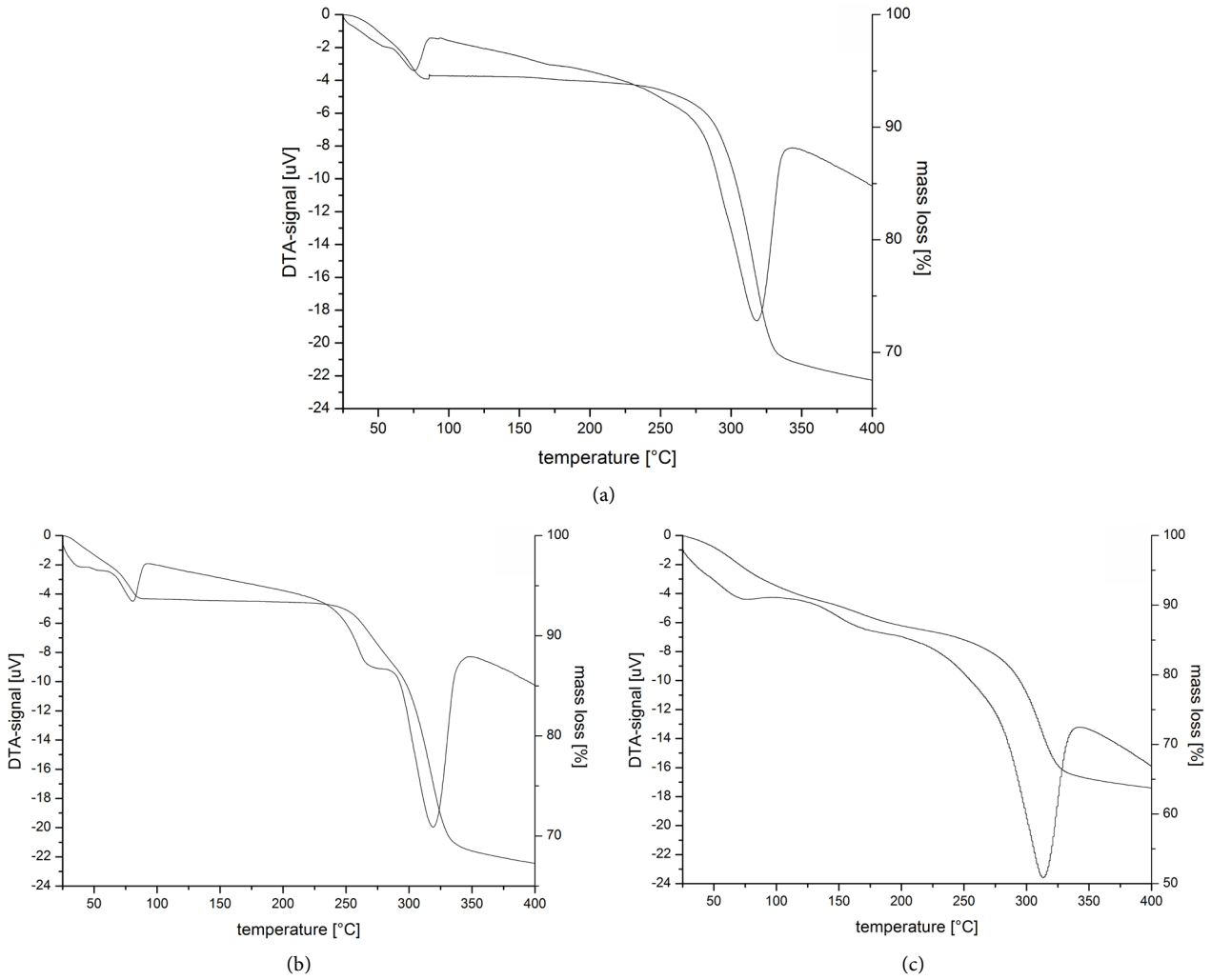

Figure 8. Thermogravimetric and differential thermal analysis of (a) $[LiAl_2(OH)_6][Cl{\cdot}0.51H_2O]$; (b) $[Li_{0.9}Mg_{0.2}Al_{1.90}(OH)_6][Cl{\cdot}0.50H_2O]$; (c) $[Mg_2Al(OH)_6][Cl{\cdot}0.55H_2O]$ (120˚C/10 h/pH 9.5/W/S 15: 1) show the loss of interlayer water at 75˚C - 100˚C). Temperatures above 275˚C destroy the structure of the main layer. Heating rate: 2.5 K/min.

Table 4. Calculated chemical formulas based on ICP-OES results and interlayer water of the solid solutions X for $[Li_{0+x}Mg_{2-2x}Al_{1+x}(OH)_6][Cl{\cdot}mH_2O]$ (120°C/10h/pH 9.5/W/S 15: 1).

X	chemical formula	interlayer water [mol]
0	$[Mg_2Al(OH)_6]Cl$	0.55
0.9	$[Li_{0.9}Mg_{0.2}Al_{1.90}(OH)_6]Cl$	0.50
0.92	$[Li_{0.92}Mg_{0.16}Al_{1.92}(OH)_6]Cl$	0.52
0.94	$[Li_{0.94}Mg_{0.12}Al_{1.94}(OH)_6]Cl$	0.50
0.96	$[Li_{0.96}Mg_{0.08}Al_{1.96}(OH)_6]Cl$	0.51
0.98	$[Li_{0.98}Mg_{0.04}Al_{1.98}(OH)_6]Cl$	0.50
1	$[LiAl_2(OH)_6]Cl$	0.51

3.2.4. FTIR Spectroscopy

To prove purity of the products, all samples were investigated by FTIR spectroscopy (**Figure 9**). Although there are 10 mol% Mg^{2+} in the solid solution, there is only a slight difference to a pure $[LiAl_2(OH)_6][Cl{\cdot}0.51H_2O]$ FTIR spectrum visible. All three spectra show the typical H_2O/OH^- absorption at ~3500 cm^{-1} and 1630 cm^{-1} [5] [18] [22] and only the spectra of $[Li_{0.9}Mg_{0.2}Al_{1.90}(OH)_6][Cl{\cdot}0.50H_2O]$ and $[Mg_2Al(OH)_6][Cl{\cdot}0.55H_2O]$ show an insignificant amount of carbonatization with the absorption at 1380 cm^{-1} [5] [18] [23]. The absorption of Al (980/720/520 cm^{-1}) related groups is very good visible for the pure Li-LDH but not as distinct for the solid solution [11] [24]. Mg related absorptions at 415 cm^{-1} are only visible in the pure Mg-LDH (**Table 5**). The amount of Mg^{2+} is high enough to influence the absorption spectra but not to show a clear Mg related absorption.

3.2.5. SEM Analysis

SEM pictures (**Figure 10**) show flat, (pseudo-) hexagonal particles with different sizes, starting at 2 - 3 µm until nearly nanosize. These particles form cluster in the size of 200 - 600 µm.

3.2.6. Structure of the Solid Solution

Based on the assumption that Mg^{2+} ions can occupy the positions of Li^+ and Al^{3+} because of the fitting bonding length [2] [21], the ion radii [7] and the determined hexagonal $P6_3/m$ space group, the structure of the pure phased solid solution should be identical with the Li-LDH (**Figure 11**). This is also indicated by the chemical composition with the formula $[Li_{0.9}Mg_{0.2}Al_{1.90}(OH)_6][Cl{\cdot}0.50H_2O]$. If Mg^{2+} ions could not enter one of the two octahedral positions, there would be two possibilities: they would exchange with Li^+ ions only, which would reduce the amount of Li^+ in the solid solution while the amount of Al^{3+} would not change, or they would exchange only with Al^{3+} ions with the opposite result. The results of this work show, that in fact Mg^{2+} has to be statistically distributed with 5 mol% on the Li^+ and 5 mol% on the Al^{3+} position to provide the measured chemical formula.

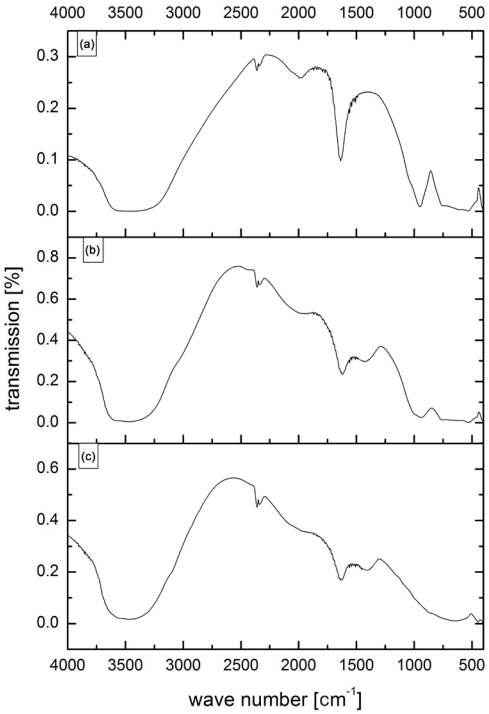

Figure 9. FTIR spectrum of (a) $[[LiAl_2(OH)_6][Cl{\cdot}0.51H_2O]$; (b) $[Li_{0.9}Mg_{0.2}Al_{1.90}(OH)_6][Cl{\cdot}0.50H_2O]$; (c) $[Mg_2Al(OH)_6][Cl{\cdot}0.55H_2O]$ with the typical absorbed water (~3500 cm^{-1} and 1620 cm^{-1}) and the metal-O and metal-OH vibrations (>1000 cm^{-1}). Absorption at 2400 cm^{-1} is device related.

Table 5. Observed wavenumbers and the assignment bending.

wavenumber [cm^{-1}]	assignment
3600 - 3400	ν_1, ν_3 (H_2O)
1630	$\nu(H_2O)$
1380	ν_a(C-O)
980	δ(Me-OH)
720	δ(Me-OH)
520	δ(Al-O)
415	δ(Mg-O)

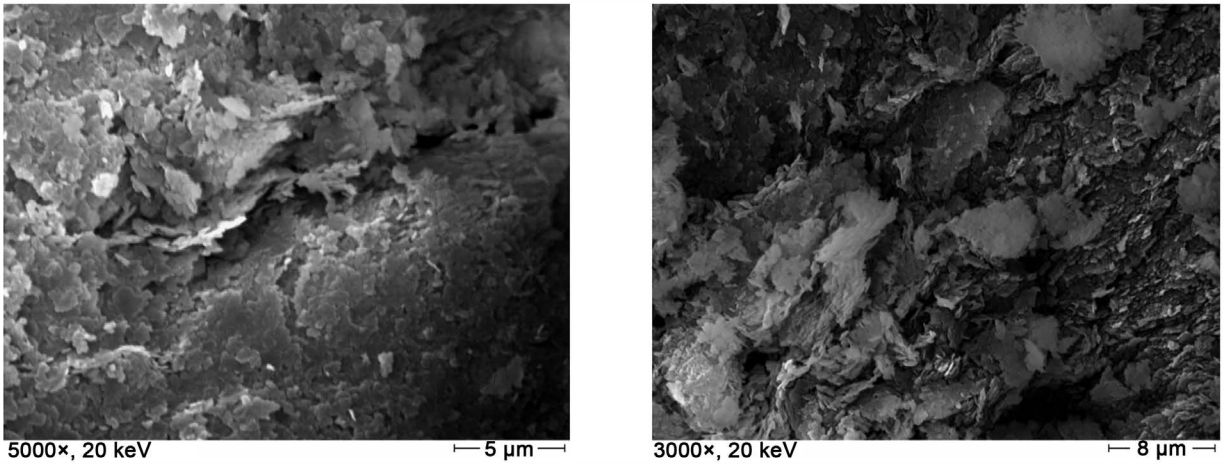

Figure 10. SEM pictures of $[Li_{0.9}Mg_{0.2}Al_{1.90}(OH)_6][Cl{\cdot}0.50H_2O]$ flat hexagonal particles with average crystal size of >3 µm.

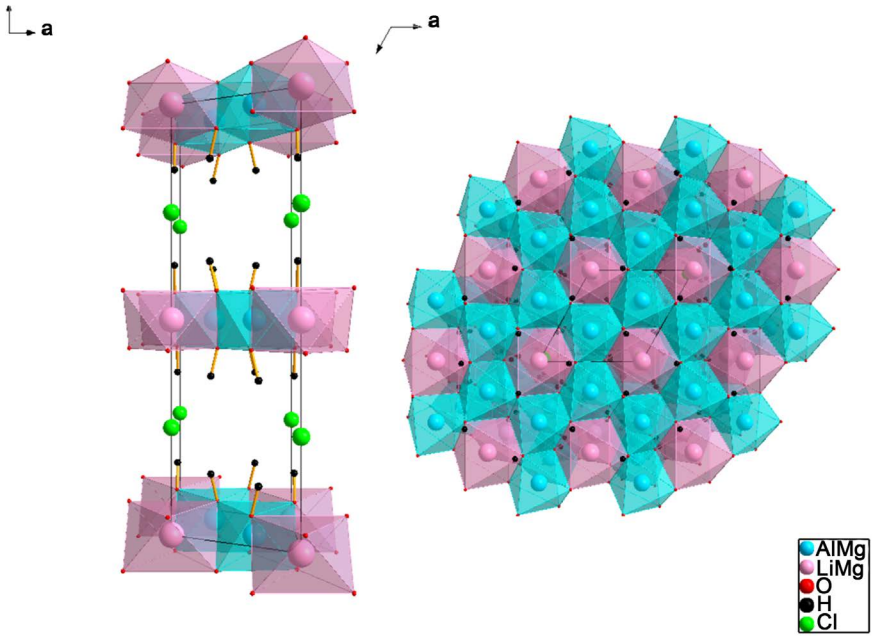

Figure 11. View of the unit cell of $[Li_{0.9}Mg_{0.2}Al_{1.90}(OH)_6]Cl{\cdot}0.5H_2O$ (based on Li-LDH structure [2]—interlayer water excluded) with the octahedral positions of Li^+ and Al^{3+}. Both positions are occupied with 5mol% by Mg^{2+}.

4. Conclusion

It is possible to synthesise a pure $[Li_{0+x}Mg_{2-2x}Al_{1+x}(OH)_6][Cl{\cdot}mH_2O]$ solid solution using autoclaves with temperatures of 100˚C, 120˚C and 140˚C with a maximum amount of 10 mol% Mg^{2+} (X = 0.9). Using more Mg^{2+} in the reactant leads to a parallel formation of an Mg^{2+} dominated and a Li^+ dominated solid solution. Optimal results for a pure solid solution can be achieved at 120˚C, pH 9.5, W/S15: 1, 10 h synthesis time. Changing the temperature to 160˚C provides the formation of an AlO(OH) phase. The pure solid solution with the highest Mg content is $[Li_{0.9}Mg_{0.2}Al_{1.9}(OH)_6][Cl{\cdot}0.50H_2O]$.

References

[1] Williams, G.R., Morrhouse, S.J., Prior, T.J., Fogg, A.M., Rees, N.H. and O'Hare, D. (2011) New Insights into the Intercalation Chemistry of $Al(OH)_3$. *Dalton Transactions*, **40**, 6012. https://doi.org/10.1039/c0dt01790f

[2] Besserguenev, A.V., Fogg, A.M., Francis, R.J., Price, S.J. and O'Hare, D. (1997) Synthesis and Structure of the Gibbsite Intercalation Compounds $[LiAl_2(OH)_6]X$ {X=Cl, Br, NO_3} and $[LiAl_2(OH)_6]Cl{\cdot}H_2O$ Using Synchrotron X-Ray and Neutron Powder Diffracion. *Chemistry of Materials*, **9**, 241-247. https://doi.org/10.1021/cm960316z

[3] Khan, A.I. and O'Hare, D. (2002) Intercalation Chemistry of Layered Double Hydroxides: Recent Developments and Applications. *Journal of Materials Chemistry*, **12**, 3191-3198. https://doi.org/10.1039/B204076J

[4] Lei, L., Millange, F., Walton, R.I. and O'Hare, D. (2000) Efficient Separation of Pyridinedicarboxylates by Preferential Anion Exchange Intercalation in $[LiAl_2(OH)_6]Cl{\cdot}H_2O$. *Journal of Materials Chemistry*, **10**, 1881-1886. https://doi.org/10.1039/b002719g

[5] Williams, G.R., Dunbar, T.G., Beer, A.J., Fogg, A.M. and O'Hare, D. (2006) Intercalation Chemistry of the Novel Layered Double Hydroxides $[MAl_4(OH)_{12}](NO_3)_2{\cdot}yH_2O$ (M=Zn, Cu, Ni and Co). 1: New Organic Intercalates and Reaction Mechanisms. *Journal of Materials Chemistry*, **16**, 1222-1230. https://doi.org/10.1039/b514874j

[6] Lei, L., Vijayan, R.P. and O'Hare, D. (2001) Preferential Anion Exchange Intercalation of Pyridinecarboxylate and Toluate Isomers in the Layered Double Hydroxide $[LiAl_2(OH)_6]Cl{\cdot}H_2O$. *Journal of Materials Chemistry*, **11**, 3276-3280. https://doi.org/10.1039/b102754a

[7] Newman, S.P. and Jones, W. (1998) Synthesis, Characterization and Applications of Layered Double Hydroxides Containing Organic Guests. *New Journal of Chemistry*, 105-115. https://doi.org/10.1039/a708319j

[8] Ragavan, A., Williams, G.R. and O'Hare, D. (2009) A Thermodynamically Stable Layered Double Hydroxide Heterostructure. *Journal of Materials Chemistry*, **19**, 4211-4216. https://doi.org/10.1039/b822390d

[9] Isupov, V.P., Chupakhina, L.E., Mitrofanova, R.P. and Tarasov, K.A. (2000) Synthesis, Structure, Properties, and Application of Aluminium Hydroxide Intercalation Compounds. *Chemistry for Sustainable Development*, **8**, 121-127.

[10] Williams, G.R., Fogg, A.M., Sloan, J., Taviot-Gueho, C. and O'Hare, D. (2007) Staging during Anion-Exchange Intercalation into $[LiAl_2(OH)_6]Cl{\cdot}yH_2O$: Structural and Mechanistic Insights. *Dalton Transactions*, 3499-3506. https://doi.org/10.1039/b705753a

[11] Constantino, V.R.L. and Pinnavaia, T.J. (1995) Basic Properties of $Mg^{2+}_{1-x}Al^{3+}_x$ Layered Double Hydroxides Intercalated by Carbonate, Hydroxide, Chloride, and Sulfate Anions. *Inorganic Chemistry*, **34**, 883-892. https://doi.org/10.1021/ic00108a020

[12] Fogg, A.M., Freij, A.J. and Parkinson, G.M. (2002) Synthesis and Anion Exchange Chemistry of Rhombohedral Li/Al Layered Double Hydroxides. *Chemistry of Materials*, **14**, 232-234. https://doi.org/10.1021/cm0105099

[13] Mitchell, S., Biswick, T., Jones, W., Williams, G. and O'Hare, D. (2007) A Synchtotron Radiation Study of the Hydrothermal Synthesis of Layerd Double Hydroxides from MgO and Al_2O_3 Slurries. *Green Chemistry*, **9**, 373-378. https://doi.org/10.1039/b613795d

[14] Hu, G., Wang, N., O'Hare, D. and Davis, J. (2007) Synthesis of Magnesium Layered Double Hydroxides in Reverse Microemulsions. *Journal of Materials Chemistry*, **17**, 2257-2266. https://doi.org/10.1039/b700305f

[15] Fogg, A.M., Williams, G.R., Chester, R. and O'Hare, D. (2004) A Novel Family of Layered Double Hydroxides—$[MAl_4(OH)_{12}](NO_3)_2{\cdot}xH_2O$ (M = Co, Ni, Cu, Zn). *Journal of Materials Chemistry*, **14**, 2369-2371. https://doi.org/10.1039/B409027F

[16] Aimoz, L., Taviot-Gueho, C., Churakov, S.V., Chukalina, M., Dähn, R., Curti, E., Bordet, P. and Vespa, M. (2012) Anion and Cation Order in Iodide-Bearing Mg/Zn-Al Layered Double Hydroxides. *The Journal of Physical Chemistry C*, **116**, 5460-5475. https://doi.org/10.1021/jp2119636

[17] Taviot-Gueho, C., Feng, Y., Faour, A. and Leroux, F. (2010) Intercalation Chemistry in a LDH System: Anion Exchange Process and Staging Phenomenon Investigated by Means of Time-Resolved, *in Situ* X-Ray Diffraction. *Dalton Transactions*, **39**, 5994-6005. https://doi.org/10.1039/c001678k

[18] Boclair, J.W., Braterman, P.S., Jiang, J., Lou, S. and Yarberry, F. (1999) Layered Double Hydroxides Stability. 2. Formation of Cr(III)-Containing Layered Double Hydroxides Directly from Solution. *Chemistry of Materials*, **11**, 303-307.

https://doi.org/10.1021/cm980524m

[19] Williams, G.R., Dunbar, T.G., Beer, A.J., Fogg, A.M. and O'Hare, D. (2005) Intercalation Chemistry of the Novel Layered Double Hydroxides $[MAl_4(OH)_{12}](NO_3)_2{\cdot}yH_2O$ (M = Zn, Cu, Ni and Co). 2: Selective Intercalation Chemistry. *Journal of Materials Chemistry*, **16**, 1231-1237. https://doi.org/10.1039/b514875h

[20] Williams, G.R. and O'Hare, D. (2006) Towards Understanding, Control and Application of Layered Double Hydroxide Chemistry. *Journal of Materials Chemistry*, **16**, 3065-3074. https://doi.org/10.1039/b604895a

[21] Bellotto, M., Rebours, B., Clause, O., Lynch, J., Bazin, D. and Elkaim, E. (1996) A Reexamination of Hydrotalcite Crystal Chemistry. *The Journal of Physical Chemistry*, **100**, 8527-8534. https://doi.org/10.1021/jp960039j

[22] Pöllmann, H., Stöber, S. and Stern, E. (2006) Synthesis, Characterizaion and Reaction Behaviour of Lamellar AFm Phases with Aliphatic Sulfonate-Anions. *Cement and Concrete Research*, **36**, 2039-2048. https://doi.org/10.1016/j.cemconres.2006.06.008

[23] Cavani, F., Trifiro, F. and Vaccari, A. (1991) Hydrotalcite-Type Anionic Clays: Preparation, Properties and Applications. *Catalysis Today*, **11**, 173-301. https://doi.org/10.1016/0920-5861(91)80068-K

[24] Dutta, P.K. and Puri, M. (1989) Anion Exchange in Lithium Aluminate Hydroxides. *The Journal of Physical Chemistry*, **93**, 376-381. https://doi.org/10.1021/j100338a072